Remote Sensing of Environment xxx (2009) xxx–xxx

Contents lists available at ScienceDirect

Remote Sensing of Environment

journal homepage: www.elsevier.com/locate/rse

Landscape-scale patterns of forest pest and pathogen damage in the Greater Yellowstone Ecosystem

Jaclyn A. Hatala [a,*], Robert L. Crabtree [b], Kerry Q. Halligan [c,1], Paul R. Moorcroft [d]

[a] Department of Environmental Science, Policy, and Management, University of California Berkeley, Berkeley, California 94720, USA
[b] Yellowstone Ecological Research Center, Bozeman, Montana 59718, USA
[c] Sanborn Map Company, 610 SW Broadway, Suite 310, Portland, OR 97205, USA
[d] Department of Organismic and Evolutionary Biology, Harvard University, Cambridge, Massachusetts 02138, USA

ARTICLE INFO

Article history:
Received 23 April 2009
Received in revised form 27 August 2009
Accepted 20 September 2009
Available online xxxx

Keywords:
Blister rust
Mountain pine beetle
Whitebark pine
Remote sensing
Ripley's *K*

ABSTRACT

Pathogen and pest outbreaks are recognized as key processes in the dynamics of Western forest ecosystems, yet the spatial patterns of stress and mortality are often complex and difficult to describe in an explicit spatial context, especially when considering the concurrent effects of multiple agents. Blister rust, a fungal pathogen, and mountain pine beetle, an insect pest, are two dominant sources of stress and mortality to high-altitude whitebark pine within the Greater Yellowstone Ecosystem (GYE). In whitebark pine populations infested with blister rust or mountain pine beetle, the shift from green to red needles at the outer-most branches is an early sign of stress and infestation. In this analysis, we investigated a method that combines field surveys with a remote sensing classification and spatial analysis to differentiate the effects of these two agents of stress and mortality within whitebark pine. Hyperspectral remotely sensed images from the airborne HyMap sensor were classified to determine the locations of stress and mortality in whitebark pine crowns through sub-pixel mixture-tuned matched-filter analysis in three areas of the GYE in September 2000 and July 2006. Differences in the spatial pattern of blister rust and mountain pine beetle infestation allowed us to separate areas dominated by mountain pine beetle versus blister rust by examining changes in the spatial scale of significant stress and mortality clusters computed by the Ripley's *K* algorithm. At two field sites the distance between clusters of whitebark pine stress and mortality decreased from 2000 to 2006, indicating domination by the patchy spatial pattern of blister rust infestation. At another site, the distance between significant stress and mortality clusters increased from 2000 to 2006, indicating that the contiguous pattern of mountain pine beetle infestation was the primary source of disturbance. Analysis of these spatial stress and mortality patterns derived from remote sensing yields insight to the relative importance of blister rust and mountain pine beetle dynamics in the landscape.

1. Introduction

Pathogen and pest outbreaks play an important role in governing the dynamics of forest ecosystems since they can dramatically alter the composition and structure of forest communities (Moorcroft et al., 2001; Tomback & Resler, 2007), which subsequently create feedback effects to patterns of fire and nutrient cycling (Castello et al., 1995; Dale et al., 2001; Logan et al., 2003). Within the Greater Yellowstone Ecosystem (GYE), whitebark pine (*Pinus albicaulis*) is considered a keystone species by conservation ecologists that is critical to trophic functionality (Tomback et al., 2001). Whitebark pine plays an essential role in altering treeline micro-climate, paving the way for the establishment of other animal, insect, plant, fungal and microbial species, and whitebark pine is an important structural component of snowpack regulation within Western watersheds (Harris, 1999; Logan & Powell, 2001). Most whitebark pine is propagated from the seed caches of the Clark's nutcracker (*Nucifraga columbiana*) (Hutchins & Lanner 1982; Tomback, 1982), and these whitebark pine nut caches of concentrated proteins and lipids are often raided by grizzly bears (*Ursus arctos*) as a critical pre-hibernation food source (Mattson et al., 1991). In years with poor whitebark pine crops, human–bear conflict often increases as grizzly bears began searching for food from other sources, and a decline in grizzly bear populations during the past ten years has been partially attributed to the decimation of whitebark pine populations in protected ecosystems south of Canada (Mattson et al., 1992).

The effects of the blister rust fungus (*Cronartium ribicola*) and mountain pine beetle (*Dendroctonus ponderosae*) dominate stress and mortality in whitebark pine populations of the Greater Yellowstone Ecosystem (Tomback et al., 2001). The mountain pine beetle is a native insect pest, while blister rust is an invasive fungal pathogen

* Corresponding author.
E-mail address: jhatala@post.harvard.edu (J.A. Hatala).
[1] Formerly with Yellowstone Ecological Research Center, Bozeman, Montana 59718, USA.

0034-4257/$ – see front matter © 2009 Elsevier Inc. All rights reserved.
doi:10.1016/j.rse.2009.09.008

specific to five-needled pines that was introduced to North America in 1910 and to the GYE more recently (Maloy, 1997). Mountain pine beetles cause mortality by boring paths through vascular tissue (Miller & Keen, 1960), and establish a colony within a forest population when a host tree becomes infected and aggregates a sufficient number of individuals to overcome tree defenses and establish a brood population, which results in the reemergence of adults at a rate of about 90 individuals per square foot, killing the entire tree in the process (Coulson, 1979). The mountain pine beetle is not specific to five-needled or whitebark pine, and can reside in other pine species in the GYE. Recovery from mountain pine beetle infestation in whitebark pine is seldom possible, and mountain pine beetles tend to kill mature whitebark pine trees within the span of one to three years, turning the entire tree crown red in the process.

Blister rust populations persist through two alternate hosts during a five-stage life cycle in the GYE: whitebark pine and one of several species in the genus *Ribes* (Mielke, 1943). Two spore stages (aeciospores and pycniospores) persist on the pines, and the other three (basidiospores, teliospores, and urediospores) propagate on *Ribes*. A whitebark pine becomes infected with blister rust when basidiospores produced on *Ribes* enter through the stomata of its needles (Agrios, 1997). This life history strategy makes blister rust difficult to both control and predict since the pathogen does not spread from tree to tree, but instead through wind-borne spores from the population of its alternate host. The huge range of spatial scales inherent in the spread of blister rust, from the microscopic spore scale to the macroscopic ecosystem scale have created difficulties in analyzing its pathology. Blister rust acts more slowly than mountain pine beetle within whitebark pine trees, causing inevitable whitebark pine mortality within a span of fifteen to twenty years. Although blister rust and mountain pine beetle co-occur within the landscape of the GYE, we hypothesize that areas dominated by blister rust stress and mortality will exhibit a pattern of patchy infestation due to the wind dispersal of spores from *Ribes* populations, which creates a pattern markedly different from an outbreak of mountain pine beetle (*Dendroctonus ponderosae*), which instead spreads directly from tree to tree, typically creating a contiguous pattern of mortality at a scale of less than 1 km during outbreaks (Logan et al., 1998).

Monitoring the effects of mortality caused by pests and pathogens has been a crucial task for U.S. forest managers since the catastrophic scale of the chestnut blight in the early twentieth century, but monitoring multiple mortality agents acting concurrently on the landscape is a spatially and temporally complex task. While plot-level forest pest and pathogen studies are collected in small-scale detail and most large-scale remote sensing studies categorize the extent of general mortality throughout the landscape, there is a strong desire to develop and use methodologies that bridge these two scales in order to develop monitoring tools that are more tractable for forest managers and more informative for tracking changes in the landscape through time and predicting future disturbance patterns. Remote sensing is an ideal tool for monitoring the activity of pests and pathogens at multiple scales, especially when considering its utility for monitoring conditions on a continuous spatial surface in remote areas with difficult access (Roughgarden et al., 1991; Booth & Cox, 2008). While the remote sensing of forest mortality in conifer-dominated ecosystems through numerous platforms has proven successful (Boyer et al., 1988; Everitt et al., 1999; Kelly & Meentemeyer, 2002; White et al., 2004; Bone et al., 2006; Wulder et al., 2006; Guo et al., 2007) including studies classifying mountain pine beetle stress and mortality (Skakun et al., 2003; Coops et al., 2006), we could find no studies to date that have attributed results from the classification of canopy stress to more than a single cause of stress and mortality in the landscape. Pest and pathogen field studies necessarily focus on the plot level and are used to extrapolate through the landscape. The 2 to 4-meter spatial scale of the HyMap sensor allows for a continuous monitoring footprint that is a close match to the spatial scale of blister rust and mountain pine beetle stress and mortality within individual trees. While the spatial footprint of HyMap imagery is smaller than that of coarser-resolution remote sensing platforms such as Landsat, the ability to monitor small-scale changes in ground conditions makes it ideal for analyzing pest and pathogen infection patterns where the key to intervention is early detection. The spatial extent and scale of the HyMap sensor provides an ideal link between small-scale forest inventories and larger scale remote sensing imagery. For example, the methodology presented in this analysis could be used in conjunction with larger scale imagery such as Landsat to potentially scale up the classification of stress and mortality. However, HyMap was considered an ideal platform for our analysis due to its small spatial scale and ability to detect small levels of stress and mortality at the branch level. Through the analysis of HyMap imagery, this paper provides a method for determining the relative contribution of blister rust and mountain pine beetle at three sites within the whitebark pine landscape of the GYE.

2. Methods

2.1. Study area and field data

This analysis used reflectance data from the HyMap (Sydney, Australia: HyVista Corporation) airborne hyperspectral sensor, which records spectral data at 126 continuous bandwidths and has a spatial resolution of 2–4 m, depending on the sensor altitude. The HyMap sensor was flown over three areas of known whitebark pine stress and mortality in the GYE on 17 October 2000, and again on 4 July 2006 (Fig. 1). We assumed in this analysis that there is no seasonal variation in the red-needle indicators of blister rust and mountain pine beetle damage between October and July. These three sites were selected for the collection of hyperspectral imagery in consultation with forest managers from the National Park Service, the U.S. Forest Service, and the USGS Northern Rocky Mountain Research Center. Sites were selected for HyMap data collection to include large amounts of whitebark pine habitat outside of Yellowstone National Park with varying levels of known blister rust and/or mountain pine beetle infestation. Other than a small amount of background mortality from events such as winter storms, forest managers identified blister rust and mountain pine beetle as the only known widespread causes of stress and mortality within whitebark pine within this region. The Daisy Pass site was selected for its absence of blister rust and mountain pine beetle infestation during preliminary field investigations during the summer of 2000. The Tom Miner and Red Lodge sites were selected due to their low level of stress and mortality signs within whitebark pine during the summer of 2000. The average elevations of Daisy Pass, Red Lodge, and Tom Miner are 2706 m, 2504 m, and 2612 m, respectively.

Within each footprint of hyperspectral imagery at the three sites, three representative whitebark pine stands with varying levels of blister rust were identified within the Daisy Pass and Red Lodge site footprints and two representative stands were identified within the Tom Miner site footprint. These representative stands, each approximately 300–500 m^2 in size, were located by field visits to the three site footprints in fall 2000. Within each of these representative stands, ten randomly located 5.2-meter radius field plots (80 plots in total) were established in fall 2000 to evaluate the absence or presence and cause of stress and mortality of each individual tree within the field plot. These field plots were all revisited in June and July 2007. In our analysis, we assume that there are no large seasonal variations between early summer and early fall (when our field surveys were conducted) for blister rust or mountain pine beetle symptoms in whitebark pine trees.

Field plots were located with Trimble XT and Trimble 3 GPS units with sub-meter accuracy in both 2000 and 2007. At each field plot located with the Trimble GPS unit, a digital photograph of the tree

Please cite this article as: Hatala, J.A., et al., Landscape-scale patterns of forest pest and pathogen damage in the Greater Yellowstone Ecosystem, *Remote Sensing of Environment* (2009), doi:10.1016/j.rse.2009.09.008

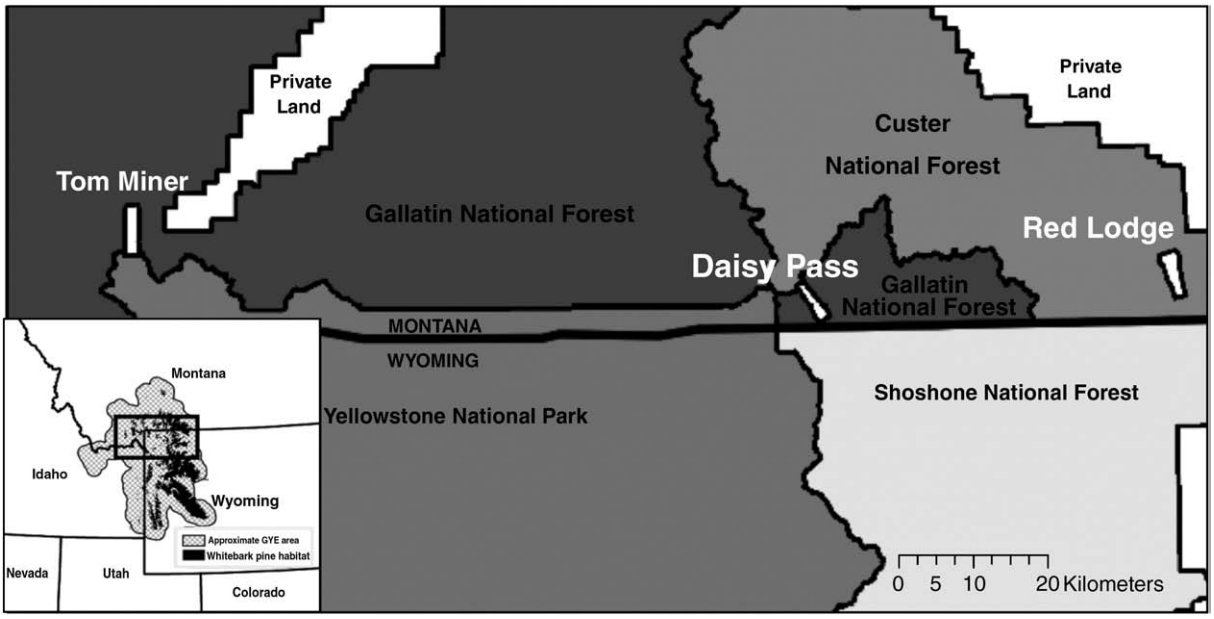

Fig. 1. The three footprints of the HyMap imagery, Tom Miner, Daisy Pass, and Red Lodge, lie just north of Yellowstone National Park, within the boundary of the Greater Yellowstone Ecosystem. The three sites were selected in consultation with the National Forest Service and the National Park Service to encompass areas of high whitebark pine content and absent to moderate levels of whitebark pine stress.

crown was collected to visually depict the actual amount of red/dead needles (Fig. 2). Individual tree data was collected for each field plot by placing every tree in the plot within one of four health classes: healthy (needles abundant and green), stressed (needles discolored), dead (all or nearly all needles red), or snag (needles absent). In addition, signs of blister rust infection (cankers, rodent chewing and fruiting bodies) as well as signs of mountain pine beetle infestation (beetle holes and sapping out) were recorded for each tree. From these field plots, five plots within each of the hyperspectral footprints (15 plots in total) were chosen for the classification of whitebark pine stress and mortality, and the remainder of the field plots (64 plots in total) is used for the validation of the imagery classification, both described below.

2.2. Pre-analysis processing of imagery

Prior to our analysis, radiometric error was corrected to onboard calibration data with the ATREM software package (Boulder, CO: University of Colorado, Cooperative Institute for Research in the Environmental Sciences) and was followed by spectral smoothing with EFFORT software (Boardman, 1998) in ENVI (Boulder, CO: ITT Visual Information Solutions) to minimize noise in the final reflectance spectra. Geometric distortion during HyMap data collection was corrected by onboard GPS measurements of the *x*, *y*, and *z* coordinates of the sensor and through inertial motion unit measurements of the pitch, yaw and roll of the aircraft. Residual geometric error was corrected by manual georegistration of the 2000 HyMap images to 1-meter resolution digital orthophoto quarter-quadrangles (USGS, 2001) and then georegistration of the 2006 HyMap imagery to the 2000 images for each site.

To focus the classification process on pixels with possible stress and mortality, a spectral mask was created to eliminate pixels dominated by non-target wavelengths. The mask limits the analysis according to two wavelength parameters: the NDVI (normalized difference between red and infrared reflectance) should fall between 0.2 and 1.0 to eliminate pixels dominated by snow, water and light-colored soils, and the short-wave infrared reflectance should be no greater than 15% to exclude pixels dominated by dark-colored soils. It is possible that this mask may have erroneously eliminated the spectra of some entirely dead trees due to the large amounts of bare soil that could be included within their spectral signature. However, the benefit to the classification process from the elimination of non-vegetation ground materials far outweighs the minimal exclusion of some dead pixels.

Rather than analyzing the entire breadth of the 126 HyMap bands, a minimum noise fraction (MNF) transform was applied to each image in order to reduce the data size and portray only the most distinguishing spectral characteristics of each image (Green et al., 1988). An MNF transform is similar to applying a principle component analysis (PCA) to each image, but whereas PCA condenses data by maximizing variance, an MNF transform uses the breadth of spectral wavelengths collected by the HyMap sensor to reduce data by maximizing the signal-to-noise ratio. Conducting an MNF transform before mixture-tuned matched-filter classification has a proven ability in increasing the producer's accuracy (Mundt et al., 2005). An MNF transform results in an image where variance within the image has been reduced to a smaller number of bands, facilitating distinction between features within the scene. In this case, 25 MNF-transformed bands were included in the analysis.

2.3. Mapping stress and mortality by the MTMF algorithm

In this analysis we use the mixture-tuned matched-filter (MTMF) algorithm to classify HyMap images for whitebark pine stress and mortality. The MTMF algorithm has been successfully used with hyperspectral imagery to classify different soil types (Lewis et al., 2008), map different plant species (Dehaan et al., 2007), compute post-fire burn severity (Robichaud et al., 2007), analyze vegetative indicators of salinization (Dehaan & Taylor, 2003), map invasive plant species (Glenn et al., 2005; Noujdina & Ustin, 2008) and monitor the pathogen infiltration of powdery mildew and leaf rust in agricultural stands of winter wheat (Franke & Menz, 2007).

In this analysis, HyMap images were classified for whitebark pine crown stress and mortality through spectral classification methods first established in Halligan et al. (2003). The spectral qualities of chlorophyll and water dominate the reflectance of healthy whitebark pine, while the structural materials cellulose and lignin dominate the canopy reflectance of whitebark pines exhibiting stress and mortality (Fig. 3). Accordingly, reference spectra for stress and mortality were

Please cite this article as: Hatala, J.A., et al., Landscape-scale patterns of forest pest and pathogen damage in the Greater Yellowstone Ecosystem, *Remote Sensing of Environment* (2009), doi:10.1016/j.rse.2009.09.008

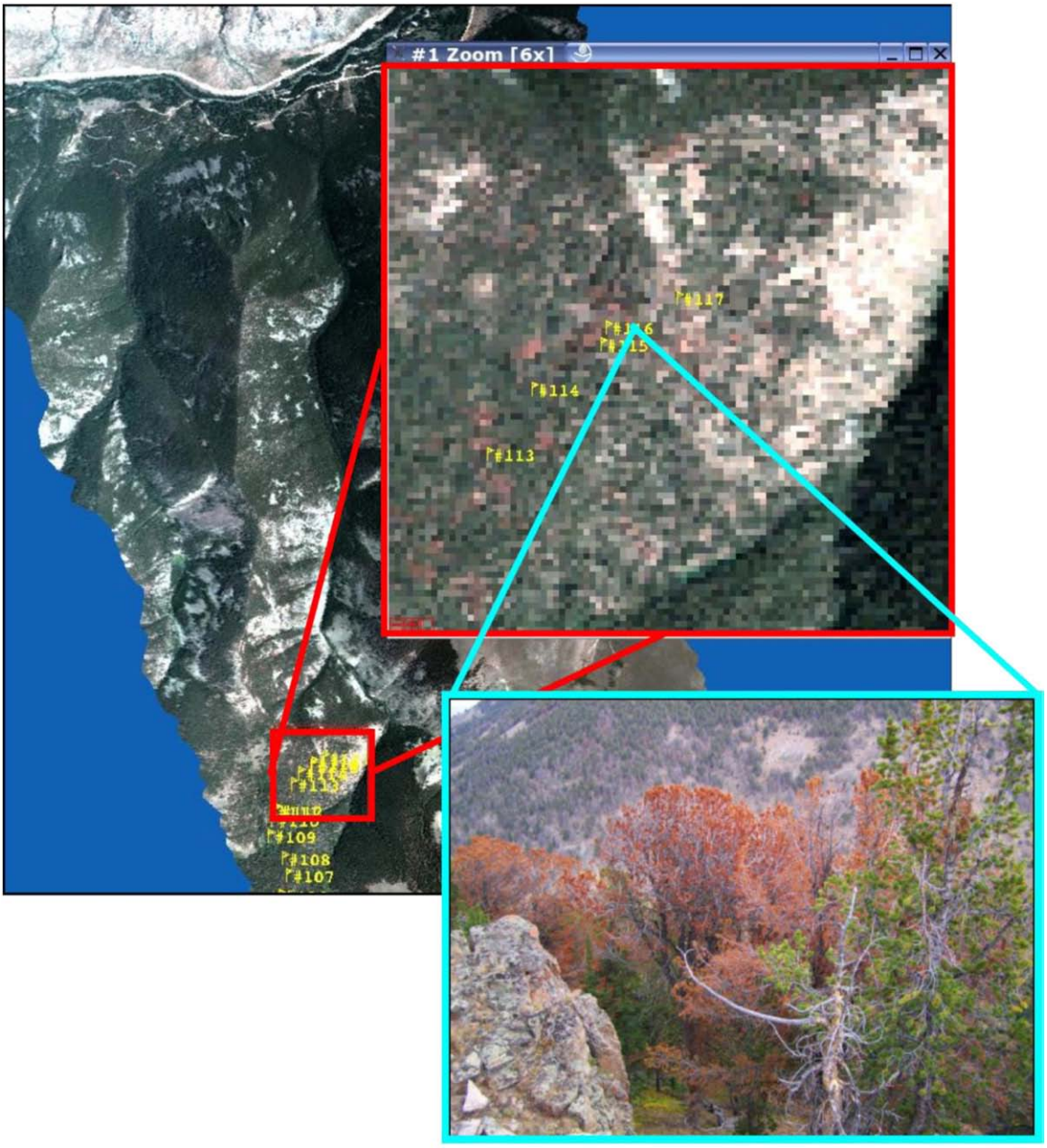

Fig. 2. An example of ground-collected GPS-tagged digital photographs to collect the reference spectrum for red/dead needles in whitebark pine crowns. This field data was collected at the Red Lodge site in August 2006.

collected from five field plots encompassing varying levels of crown stress and mortality within each of the three hyperspectral images (15 training plots in total). These field plots in total provided 8–10 stress and mortality training pixels per image in 2000 and 14 stress and mortality training pixels per image in 2006. All training pixels used in the classification are unique to the site footprint and year in which they were collected. Mean pixel values were calculated from each training pixel to derive the reference spectrum for stress and mortality within that image.

The identification of whitebark pine stress and mortality was computed by the MTMF algorithm, which is a form of spectral mixture analysis that unmixes pixels and matches pixels in the image to the endmember spectra by maximizing the target response and minimizing background spectral signatures. The MTMF algorithm consists of two steps. First, a set of training pixels was used to define the characteristic reference spectrum for whitebark pine stress and mortality. Second, all pixels in the image containing a portion of the reference spectrum are spectrally unmixed and classified. The MTMF algorithm is described by:

$$\vec{r}_{ij} = \vec{d}\alpha + \vec{U}\gamma + n \quad (1)$$

where $\vec{r}$ represents the spectral signature of the pixel at location i,j, $\vec{d}$ is the spectrum of the target to be mapped (in this case the image reference spectra for stress and mortality), α is the abundance fraction of the desired endmember, $\vec{U}$ represents the mixed spectrum of undesired endmembers, γ is the abundance fraction of undesired spectral endmembers, and n is Gaussian noise (Harsanyi & Chang, 1994). The MTMF algorithm was constrained so that abundance fractions are positive and solved for the abundance fraction of the desired endmember in each pixel throughout the image. Computation of the MTMF resulted in an output image with two component vectors: *matched-filter score* that describes the abundance fraction of the target endmember, and *infeasibility* that quantifies the noise for each pixel in

Please cite this article as: Hatala, J.A., et al., Landscape-scale patterns of forest pest and pathogen damage in the Greater Yellowstone Ecosystem, *Remote Sensing of Environment* (2009), doi:10.1016/j.rse.2009.09.008

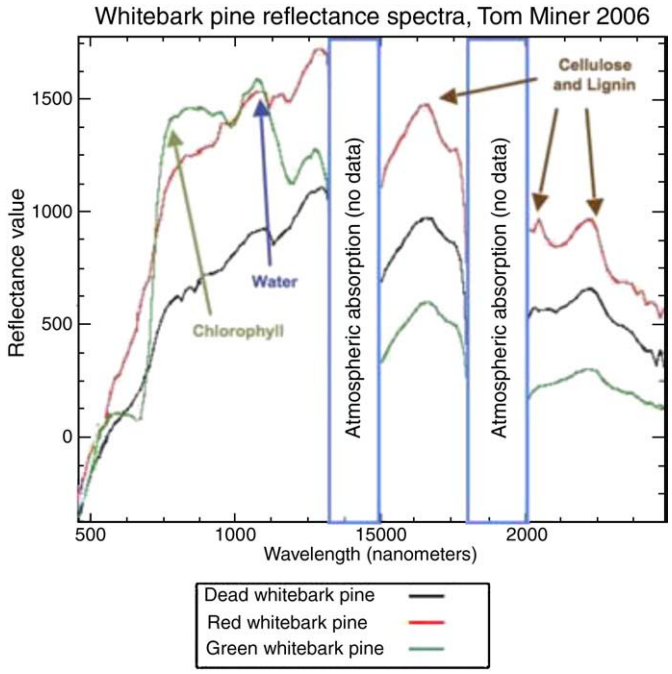

Fig. 3. Spectral classification of red/dead flagging in whitebark pine is possible because of differences in the reflectance spectra of green, red and dead whitebark pine crowns derived from the imagery of the HyMap sensor. Differences between the reflectance properties of chlorophyll, water, cellulose and lignin create distinguishing spectra for the three different classes of whitebark pine stress.

units that scale with the matched-filter score (higher target endmember abundance fractions have lower noise variance). The two component output images of infeasibility and the matched-filter score were then thresholded to maximize the inclusion of true red/dead pixels (maximizing matched-filter score) and minimize the inclusion of false positives (minimizing infeasibility). A threshold was selected for each image that attempted to achieve maximum classification accuracy by selecting 80% of the pixels that fell on either side of a 1:1 plot of matched-filter score versus infeasibility for each image. This threshold was computed separately for the stressed class and the dead class for each image.

Within this analysis, stress and mortality are merged into one class post-classification, and the spectral abundance fractions are converted into the binary presence or absence of stress and mortality. We merge the two classes of stress and mortality in this study in order to apply a spatial analysis that investigates the total effects of pests and pathogens within the image footprint. By merging the stress and mortality classes, we assessed the overall spatial patterns resulting from the progressive effects of the pests and/or pathogens rather than assessing solely the pattern of stress or mortality.

2.4. Classification assessment

Excluding the five field plots from each of the three hyperspectral footprints used in the MTMF classification process, the remainder of the field plots (64 total plots) established in 2000 and revisited in 2007 are used for the classification assessment of the MTMF stress and mortality mapping. The classification error for stress and mortality was calculated by taking into account both errors of commission (erroneous inclusion of pixels) and errors of omission (erroneous exclusion of pixels). The tree-level field data collected was classified into three categories: mapped in classification and definitely red/dead in the field (true positives), mapped and not red/dead (false positives), and unmapped and possibly red/dead (false negatives), from which producer's and user's accuracies were calculated. The producer's accuracy describes the ability of a classification scheme to accurately place pixels into the desired classes and measures errors of omission, while the user's accuracy describes the probability that a sample from ground conditions will fall within the correct class, measuring errors of commission.

2.5. Spatial analysis

Using the MTMF stress and mortality classification with information about the life history strategies of blister rust and mountain pine beetle, we used spatial statistics to separate the spatial mortality patterns of blister rust and mountain pine beetle operating in the same ecosystem. As we show here, once stress and mortality patterns are classified across the landscape through remotely sensed imagery, it is possible to use the spatial statistical approach of the Ripley's *K* equation to analyze pathogen patterns within each of the three selected sites measured with the hyperspectral sensor in both 2000 and 2006. The Ripley's *K* function has proven utility for analyzing spatial vegetation patterns over the landscape (Haase, 1995), and has been applied to patterns of invasive species (Call & Nilsen, 2002; Suzuki et al., 2003; Deckers et al., 2005) and forest mortality (Szwagrzyk & Czerwczak, 1993; Peterson & Squiers, 1995; Moeur, 1997; Chen & Bradshaw, 1999; He & Duncan, 2000). Within studies of forest pathogens, the Ripley's *K* function has been applied to analyzing the spatial pattern of the invasive Sudden Oak Death (Kelly & Meentemeyer, 2002) as well as to analyze increased fire risk due to pathogen-induced tree mortality (Lynch et al., 2006). In this analysis, we used Ripley's *K* equation to quantify changes in the spatial extent to which whitebark pine stress and mortality in different areas arises from blister rust versus mountain pine beetle.

Ripley's *K* function (Ripley, 1976, 1981) was used to quantify the extent of spatial clustering in whitebark pine stress and mortality in each image. Ripley's *K* function is described as:

$$\hat{K}(s) = \frac{1}{\lambda^2 A}\sum_{i}^{N}\sum_{j\neq i}^{N} I_s(d_{ij}) \quad (2)$$

where for distance s at location i,j, λ is the intensity of the point process (the number of events divided by A), A is the total study area, and $I_s(d_{ij})$ is the indicator function that equals one on the distance interval d_{ij} between i and $j \leq s$ and zero on d_{ij} between i and $j > s$ (Bailey & Gatrell, 1995). Defined as the average number of events (in this case, classified stress and mortality pixels) within circles with a diameter of a defined distance interval centered on each event occurrence, divided by the mean intensity of events throughout the image, Ripley's *K* function can be used to determine the scale at which stress and mortality clustering occurs. Stress and mortality pixels within one distance event of the edge were mirrored in order to reduce edge effects inherent in executing the Ripley's *K* algorithm on a bounded point pattern (Haase, 1995; Goreaud & Pelissier, 1999). Confidence intervals for the computed Ripley's *K* function were calculated through 1000 Markov-chain Monte Carlo iterations.

The Ripley's *K* algorithm was computed for all of the six classified red/dead point patterns, and for each of the three study sites, the red/dead point pattern was constrained to the area of the 2000 HyMap footprints. When the Ripley's *K* function is plotted over distance, the line 1:1 represents a spatially random pattern, a function that exceeds the line 1:1 indicates that the pattern is spatially clustered, and a function that lies below the 1:1 line indicates a pattern that is spatially regular.

3. Results

Whitebark pine stress and mortality are mapped for all six HyMap images by the MTMF process (Fig. 4). The mixture-tuned matched-filter algorithm classified the remotely sensed images for any whitebark pine crown stress and mortality, the extent of which

Please cite this article as: Hatala, J.A., et al., Landscape-scale patterns of forest pest and pathogen damage in the Greater Yellowstone Ecosystem, *Remote Sensing of Environment* (2009), doi:10.1016/j.rse.2009.09.008

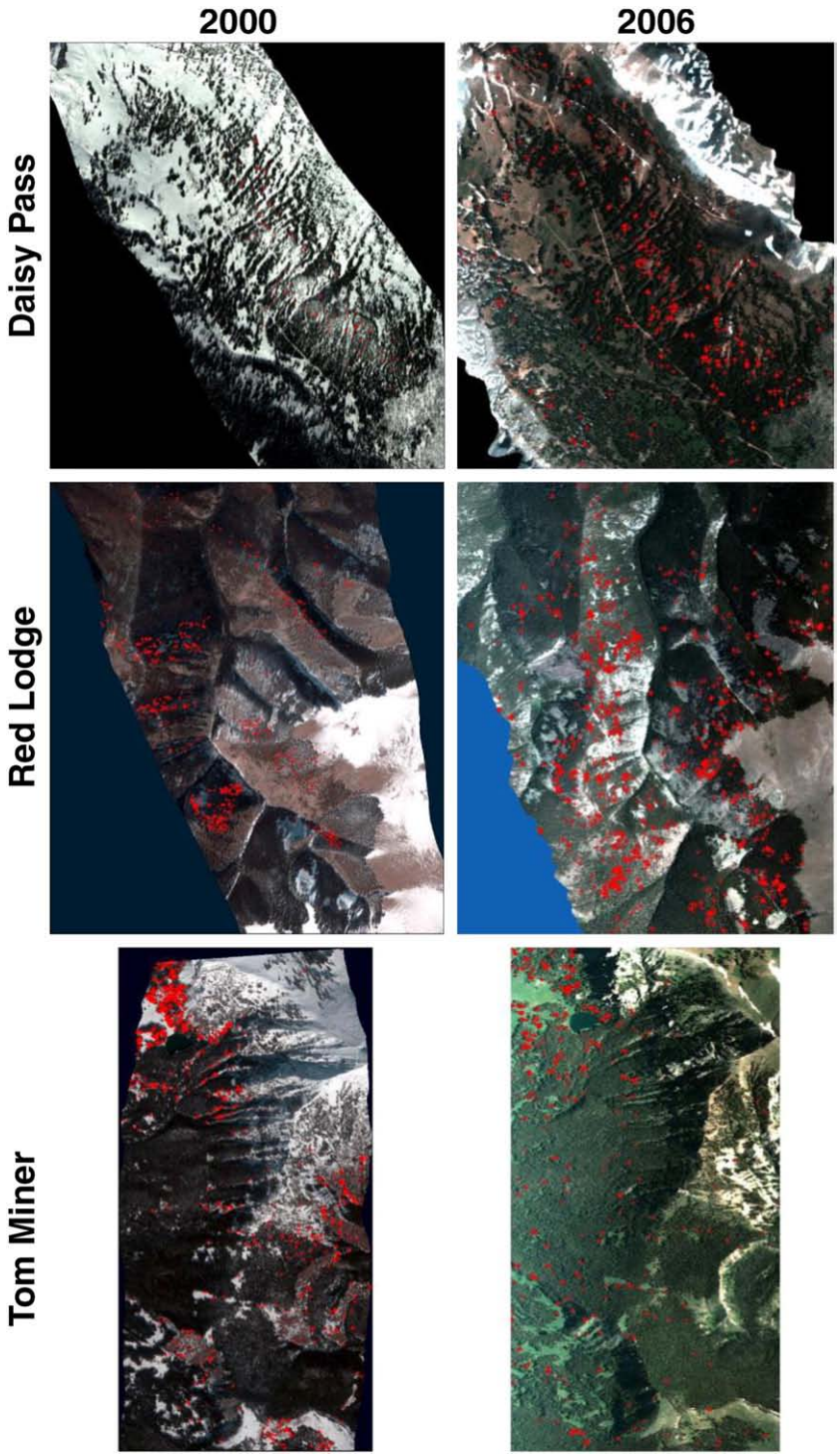

Fig. 4. The whitebark pine crown stress and mortality classification results for each of the HyMap images are here overlaid on a true-color composite of the image. Each red point represents a pixel that was classified as containing a portion of the red/dead flagging training reflectance spectrum. (For interpretation of the references to color in this figure legend, the reader is referred to the web version of this article.)

varied between sites and years. The Daisy Pass site had the least amount of classified stress and mortality, with a total of 256 pixels with crown stress and mortality in 2000 and an increase to 624 pixels in 2006, while Tom Miner had the highest number of crown stress and mortality pixels in both years, with 842 pixels of crown stress and mortality in 2000 and 1844 pixels in 2006. The Red Lodge site had an intermediate level of crown stress and mortality, with 565 pixels in 2000 and 1057 pixels in 2006. Producer's accuracy ranged from 82% to 95%, and user's accuracy ranged from 94% to 97% for the images, indicating a highly accurate classification scheme (Table 1). Accuracies were computed based on the 64 field plots not used in the MTMF classification where data was first collected in 2000 and re-collected in 2006.

From the spatial statistics executed on the point patterns of whitebark pine crown stress and mortality, all of the classified images demonstrated some level of clustering (Fig. 5); however, the degree of clustering within each of the three study sites changed differently throughout the 2000–2006 time period. At Daisy Pass, the distance at

Please cite this article as: Hatala, J.A., et al., Landscape-scale patterns of forest pest and pathogen damage in the Greater Yellowstone Ecosystem, *Remote Sensing of Environment* (2009), doi:10.1016/j.rse.2009.09.008

Table 1
The producer's and user's accuracies for whitebark pine crown stress and mortality within each HyMap scene were quite high for a remote sensing classification.

Location	Year	Producer's accuracy	User's accuracy
Daisy Pass	2000	95%	94%
	2006	94%	96%
Red Lodge	2000	82%	95%
	2006	90%	96%
Tom Miner	2000	88%	97%
	2006	93%	97%

Accuracies were computed by using the 64 field plots that were not used in the MTMF classification process where data was first collected in 2000 and re-collected in 2007. Classification accuracy for the 2006 scenes (90–97%) was generally higher than that for 2000 (82–97%). The likely explanation for this is the greater number of training polygons collected for the 2006 analysis (14 training pixels per image) compared with 2000 images (8–10 training pixels per image).

which there is no longer significant clustering (the intercept where *K*-observed crosses *K*-expected on the Ripley's *K* plots) decreases at Daisy Pass from greater than 1000 m in 2000 to 395 m in 2006. Similarly, at Red Lodge, the clustering distance changed from 587 m in 2000 to 362 m in 2006. The spatial pattern of stress and mortality at Tom Miner behaves differently than that of Daisy Pass and Red Lodge, and its Ripley's *K* function increases from a distance interval of 715 m in 2000 to a distance interval of 846 m in 2006.

The decrease in the distance of spatial aggregation at Daisy Pass and Red Lodge indicates that an overall dynamic of small-scale landscape fragmentation dominated these two sites between 2000 and 2006. This increase in small-scale heterogeneity mirrors the predicted pathology of blister rust, as it spreads from *Ribes* populations through its airborne spores to whitebark pine, effectively filling in small patches of infection throughout the landscape. The pattern at Tom Miner mirrors the pathology of mountain pine beetle, as the increase in the distance of significant clustering indicates that the pattern is dominated by the growth of a contiguous patch of mortality.

The difference in pathogenic influence of the three images is supported by ground-based measurements from the aggregated data from the field validation plots within each of the representative stands (Fig. 6). Fig. 6 represents data aggregated from all 80 field plots (10 plots per stand), where data was first collected in 2000 and re-collected in 2006. While mountain pine beetle activity was either absent or static between 2000 and 2006 at the Daisy Pass and Red Lodge sites, blister rust showed large increases between the two years. Conversely at Tom Miner, blister rust levels remained rather static from 2000 and 2006 and mountain pine beetle showed a large increase. We used a two-tailed *t*-test to determine significant increases in pathogen activity for each of the 8 sites, and found that there was a significant increase in blister rust (p-value<0.001) for all Daisy Pass sites and Red Lodge sites 1 and 2. There was a significant increase in mountain pine beetle (p-value<0.001) between years for

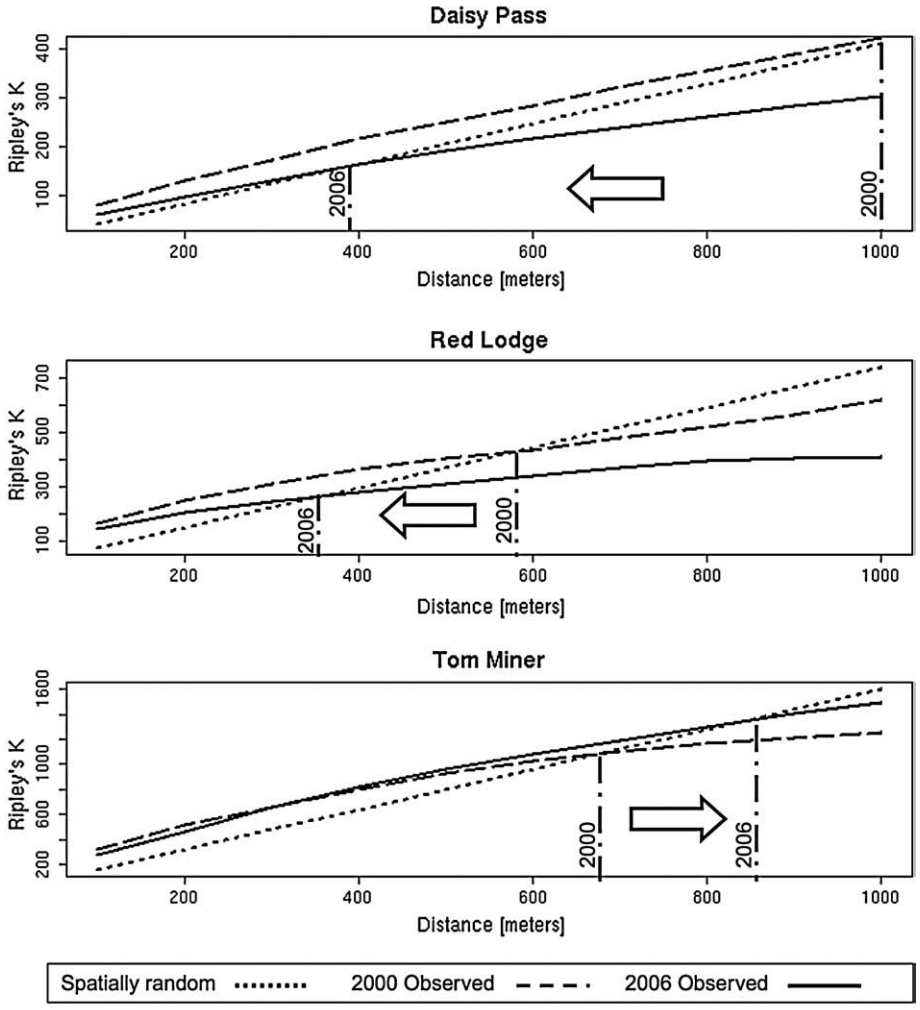

Fig. 5. The Ripley's *K* equations are computed for each of the classified stress and mortality point patterns in 2000 and 2006. The distance of significant spatial clustering (where the observed Ripley's *K* function exceeds the prediction of complete spatial randomness) decreased from 2000 to 2006 at Daisy Pass and Red Lodge, whereas the distance of significant clustering at Tom Miner increased, indicating possible differences in the cause of whitebark pine crown stress and mortality.

Please cite this article as: Hatala, J.A., et al., Landscape-scale patterns of forest pest and pathogen damage in the Greater Yellowstone Ecosystem, *Remote Sensing of Environment* (2009), doi:10.1016/j.rse.2009.09.008

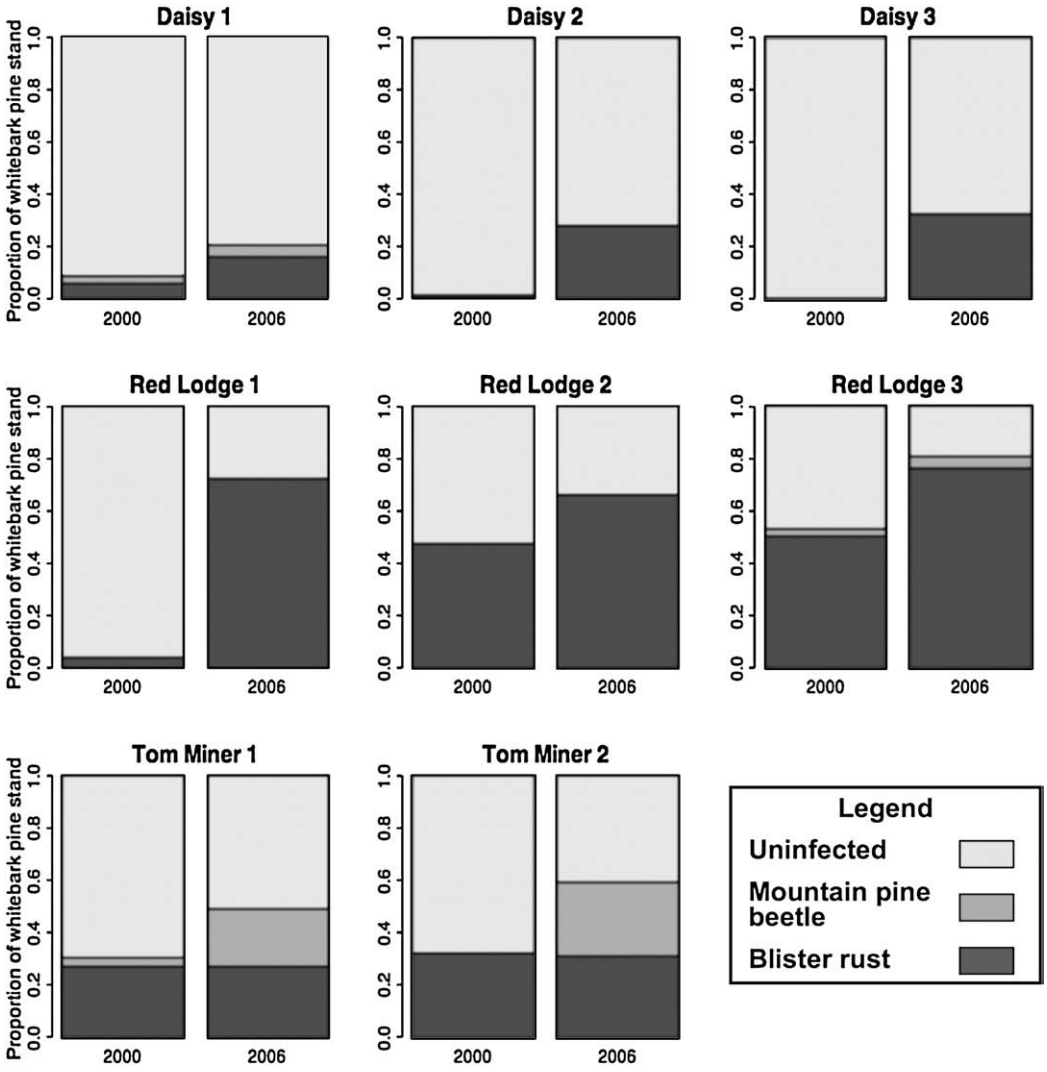

Fig. 6. This analysis contains data from 80 5.2-meter radius field inventory plots, first surveyed in 2000 and again in 2007, and supports the results from the Ripley's *K* analysis. While mountain pine beetle was absent or static at Daisy Pass and Red Lodge, blister rust increased dramatically, whereas blister rust remained static at Tom Miner and mountain pine beetle instead showed a large increase between the two years. There was a statistically significant increase between years in blister rust (p-value<0.001 in an unpaired two-tailed t-test) for all Daisy Pass sites as well as the Red Lodge 1 and 2 sites. There was a statistically significant increase between years in mountain pine beetle (p-value<0.001) for both Tom Miner sites. All other relationships between years were insignificant.

both Tom Miner sites. p-Values for all sites are included as Table 2. The field data thus directly support the inference obtained from the analysis of spatial patterns; namely that mountain pine beetle infection dominates the changing spatial pattern of infection at Tom Miner, while blister rust is responsible for the pattern of infection at Daisy Pass and Red Lodge.

Table 2
We used the two-tailed t-test to determine whether the changes in the amount of blister rust and/or mountain pine beetle were significant for all sites presented in Fig. 6.

Site	Agent	p-Value
Daisy Pass 1	Blister rust	<0.001
	Mountain pine beetle	0.637
Daisy Pass 2	Blister rust	<0.0001
	Mountain pine beetle	N/A
Daisy Pass 3	Blister rust	<0.0001
	Mountain pine beetle	N/A
Red Lodge 1	Blister rust	<0.0001
	Mountain pine beetle	N/A
Red Lodge 2	Blister rust	<0.001
	Mountain pine beetle	N/A
Red Lodge 3	Blister rust	0.0675
	Mountain pine beetle	0.3787
Tom Miner 1	Blister rust	0.7829
	Mountain pine beetle	<0.001
Tom Miner 2	Blister rust	0.8775
	Mountain pine beetle	< 0.0001

4. Discussion

Using the Ripley's *K* function to analyze the patterns of stress and mortality created by the highly accurate MTMF classification highlighted the fundamental differences in the cause of spatial fragmentation between 2000 and 2006 at the three sites. The differences in the patterns of stress and mortality parallel the differences in the underlying pathogen dynamics that govern the Tom Miner site in comparison with the Daisy Pass and Red Lodge sites. While blister rust and mountain pine beetle co-occur in the landscape, the dominance of either blister rust or mountain pine beetle dynamics can be deduced through changes within the scale of spatial aggregation over time as determined by the Ripley's *K* equation.

We used the Ripley's *K* equation to calculate the distance of significant clustering between stress and mortality points. By looking at changes in the distance of significant clustering between 2000 and 2006, we demonstrated an increasing distance of significant stress and mortality clustering as calculated by Ripley's *K*, indicating that the

Please cite this article as: Hatala, J.A., et al., Landscape-scale patterns of forest pest and pathogen damage in the Greater Yellowstone Ecosystem, *Remote Sensing of Environment* (2009), doi:10.1016/j.rse.2009.09.008

landscape is dominated by a pattern of contiguous mortality, the pattern dominant in mountain pine beetle attack. This spatial pattern of contiguous mortality parallels the predicted pattern of mountain pine beetle dynamics, as the beetles typically move to spatially proximal trees throughout the landscape and was the dominant spatial pattern at the Tom Miner site. Conversely, in a whitebark pine landscape dominated by blister rust infestation, the distance of significant stress and mortality clustering calculated by Ripley's *K* decreases over time, indicating a spatial pattern of "infilling" between infected patches. This spatial dynamic was dominant at the Daisy Pass and Red Lodge sites between 2000 and 2006.

It is important to note that landscape-level tree stress and mortality is a complex process and alternate explanations could exist for the observed differences in spatial patterns of whitebark pine fragmentation. The most convincing alternative hypothesis for the growth of a single, contiguous patch of stress and mortality is that the distribution is the result of habitat preference for blister rust, rather than the dominance of mountain pine beetle mortality. Spatial preference for the selection of blister rust infestation patterns in whitebark pine habitat could dominate the overall red/dead distribution pattern if the single, contiguous patch of stress and mortality within the Tom Miner scene is an area of whitebark pine habitat predisposed towards blister rust infection.

In our analysis we attempted to correlate presence/absence as well as level of blister rust and mountain pine beetle infestation within potential micro-climate factors including slope, elevation and aspect derived from the National Elevation Dataset (USGS, 1999). We found no significant relationships between presence/absence or level of infection with micro-climate variables within the 2000 and 2007 field datasets, within the 2000 and 2006 classified imagery, or between a 2000 and 2006 differenced change map. Further details of this environmental analysis are beyond the scope of this paper and will be presented in Hatala et al., submitted for publication.

While our analysis is limited to two time points and a limited spatial extent, using the Ripley's *K* function over time provided a fundamental first-look at the differences within the underlying spatial processes that govern the distribution of stress and mortality within these three whitebark pine sites. The method presented in this analysis can be generalized to other host–pathogen forest systems, where differences in pathogen spatial dynamics translate into different landscape fragmentation patterns. By using the Ripley's *K* equation to calculate the distance of significant clustering and how it changes over time, land managers can gain insight into the dominant causes of mortality in large continuous spatial areas throughout many landscapes. For example, a similar approach could be used to analyze a disturbed landscape that contained both the contiguous pattern of fire and the spatially heterogeneous pattern of water stress. The ability to separate and predict the causes of mortality and patterns of fragmentation is a key to predicting the effects of disturbances to the ecosystem, and this method of comparing the Ripley's *K* value over time has widespread application to landscape ecology.

5. Conclusion

Understanding increases in landscape fragmentation from the combined dynamics of blister rust and mountain pine beetle will be the key to understanding forest community dynamics at treeline within whitebark pine habitat and has wide application for predicting an interdisciplinary suite of changes in the high-altitude landscape of the GYE. Interpreting the extent and spatial dynamic of both blister rust and mountain pine beetle as was determined in this analysis is an essential first step towards understanding changes within high-altitude whitebark pine habitat as a result of these disturbances. Since whitebark pine has important connections to other organisms and ecological processes within the GYE, the increase in stress and mortality of whitebark pine within all three sites is expected to have a cascade of effects to other trophic levels. Categorizing and quantifying the dynamics of blister rust and mountain pine beetle in the landscape, will assist the selection of strategic whitebark pine stands to prioritize the replanting or conservation of blister rust-resistant whitebark pine (Schoettle & Sniezko, 2007), currently considered the most effective management strategy for dealing with blister rust.

Interest in large-scale dynamics of forest pathogen stress and mortality is increasing with concerns regarding the effects of global climate change on terrestrial ecosystems. Global climate change is expected to impact both the size and frequency of ecosystem disturbances such as forest pathogen and pest outbreaks. This further complicates the already arduous task of monitoring huge areas of land for forest managers. The methods and results of this analysis demonstrate that examining changes in the Ripley's *K* equation over time from a remote sensing classification scheme provided an accurate primary analysis of different agents of stress and mortality operating concurrently in the landscape. The methodology presented in this paper, which combined small-scale field surveys with remote sensing, provides land managers and landscape ecologists with a tool for analyzing the spatial effects of multiple agents of forest stress and mortality and can serve as an informed first-look that can be used to focus more intensive field campaigns.

Acknowledgements

We thank Larry Timchak and the Greater Yellowstone Coordinating Committee for providing funding for the hyperspectral imagery and field logistics. The NASA Biodiversity and Ecological Forecasting program also supported this research under award NNA07CN19A to Robert L. Crabtree. Ward McCaughey, Chuck Schwartz, Don Despain, and Dan Reinhart aided in the study design and selection of sites. Special thanks to Heather Lynch for her advice and support. We also acknowledge Andrew Carreras, Anne-Marie Casper, Nathan Emery, Christopher Farmer, Michael Gadsden, Allison Giguere, Amelia Hagen-Dillon, Joshua Harmsen, Laura Holtrop, Jeanine Moy, Lynette Noble, Jamie Robertson, and Jeremy Shive for their fieldwork on this project. We thank the all the staff at the Yellowstone Ecological Research Center in Bozeman, MT for their assistance with field planning and technical support while collecting data in the GYE.

References

Agrios, G. N. (1997). *Plant pathology*, 4th Edition. Orlando, FL: Academic Press.
Bailey, A., & Gatrell, T. (1995). *Interactive spatial data analysis.* New York, NY: Prentice Hall.
Boardman, J.W., 1998. Post-ATREM polishing of AVIRIS apparent reflectance data using EFFORT: a Lesson in accuracy versus precision, in Summaries of the 7th JPL Airborne Earth Science Workshop, vol. 1, JPL Pub. 97–21, p. 53.
Bone, C., Dragicevic, S., & Roberts, A. (2006). A fuzzy-constrained cellular automata model of forest insect infestations. *Ecological Modelling*, *192*, 107—125.
Booth, D. T., & Cox, S. E. (2008). Image-based monitoring to measure ecological change in rangeland. *Frontiers in Ecology and the Environment*, *6*(4), 185—190.
Boyer, M., Miller, J., Belanger, M., & Hare, E. (1988). Senescence and spectral reflectance in leave of northern pin oak (*Quercus palaustris Muenchh.*). *Remote Sensing of Environment*, *25*, 71—87.
Call, L. J., & Nilsen, E. T. (2002). Analysis of spatial patterns and spatial association between the invasive Tree-of-Heaven (Ailanthus altissima) and the native black locust (Robinia pseudoacacia). *The American Midland Naturalist*, *150*, 1—14.
Castello, J. D., Leopold, D. L., & Smallidge, P. L. (1995). Pathogens, patterns, and processes in forest ecosystems. *BioScience*, *45*, 16—24.
Chen, J., & Bradshaw, G. A. (1999). Forest structure in space: A case study of an old growth spruce-fir forest in Changbaishan Natural Reserve, PR China. *Forest Ecology and Management*, *120*, 219—233.
Coops, N. C., Wulder, M. A., & White, J. C. (2006). Integrating remotely sensed and ancillary data to characterize a mountain pine beetle infestation. *Remote Sensing of Environment*, *105*, 83—97.
Coulson, R. N. (1979). Population dynamics of bark beetles. *Annual Review of Entomology*, *24*, 417—447.
Dale, V. H., Joyce, L. A., McNulty, S., Neilson, R. P., Ayers, M. P., Flannigan, M. D., et al. (2001). Climate change and forest disturbances. *Bioscience*, *51*, 723—734.
Deckers, B., Verheyen, K., Hermy, M., & Muys, B. (2005). Effects of landscape structure on the invasive spread of black cherry (Prunus serotina) in an agricultural landscape in Flander, Belgium. *Ecography*, *28*, 99—109.

Please cite this article as: Hatala, J.A., et al., Landscape-scale patterns of forest pest and pathogen damage in the Greater Yellowstone Ecosystem, *Remote Sensing of Environment* (2009), doi:10.1016/j.rse.2009.09.008

Dehaan, R., & Taylor, G. R. (2003). Image-derived spectral endmembers as indicators of salinisation. *International Journal of Remote Sensing*, *24*, 775−794.
Dehaan, R., Louis, J., Wilson, A., Hall, A., & Rumbachs, R. (2007). Discrimination of blackberry (Rubus fruticosus sp agg.) using hyperspectral imagery in Kosciuszko National Park, NSW, Australia. *ISPRS Journal of Photogrammetry and Remote Sensing*, *62*, 13−24.
Everitt, J., Escobar, D., Appel, D., Riggs, W., & Davis, M. (1999). Using airborne digital imagery for detecting oak wilt disease. *Plant Disease*, *83*, 502−505.
Franke, J., & Menz, G. (2007). Multi-temporal wheat disease detection by multi-spectral remote sensing. *Precision Agriculture*, *8*, 161−172.
Glenn, N. F., Mundt, J. T., Weber, K. T., Prather, T. S., Lass, L. W., & Pettingill, J. (2005). Hyperspectral data processing for repeat detection of small infestations of leafy spurge. *Remote Sensing of Environment*, *95*, 399−412.
Goreaud, F., & Pelissier, R. (1999). On explicit formulas of edge effect correction for Ripley's K-function. *Journal of Vegetation Science*, *10*, 433−438.
Green, A. A., Berman, M., Switzer, P., & Craig, M. D. (1988). A transformation for ordering multispectral data in terms of image quality with implications for noise removal. *IEEE Transactions on Geoscience and Remote Sensing*, *26*, 65−74.
Guo, Q. H., Kelly, M., Gong, P., & Liu, D. S. (2007). An object-based classification approach in mapping tree mortality using high spatial resolution imagery. *GIScience and Remote Sensing*, *44*, 24−47.
Haase, P. (1995). Spatial pattern analysis in ecology based on Ripley's K function: Introduction and methods of edge correction. *Journal of Vegetation Science*, *6*, 575−582.
Halligan, K. Q., Crabtree, R. L., & Jones, M. O. (2003). Hyperspectral Data Analysis of Whitebark Pine (*Pinus albicaulis*) and White Pine Blister Rust (*Cronartium ribicola*) at Four Sites in the Greater Yellowstone Ecosystem. Unpublished report to the Greater Yellowstone Coordinating Committee, 55 pp.
Harris, J. L. (1999). Evaluation of white pine blister rust on the Shoshone National Forest. *USDA Forest Service Rocky Mountain Region, Biological Evaluation R2-99-05*.
Harsanyi, J. C., & Chang, C. -I. (1994). Hyperspectral image classification and dimensionality reduction: An orthogonal subspace projection approach. *IEEE Transactions on Geoscience and Remote Sensing*, *32*, 779−784.
Hatala, J. A., Dietze, M. C., Crabtree, R. L., the Interagency Whitebark Pine Monitoring Working Group, Kendall, K. D. Six, et al., (submitted for publication). An ecosystem-scale model of white pine blister rust (*Cronartium ribicola*) spread in whitebark pine (*Pinus albicaulis*) of the Greater Yellowstone Ecosystem. Submitted to *Ecological Applications*.
He, F., & Duncan, R. P. (2000). Density-dependent effects on tree survival in an old-growth Douglas fir forest. *Journal of Ecology*, *88*, 676−688.
Hutchins, H. E., & Lanner, R. M. (1982). The central role of Clark's nutcracker in the dispersal and establishment of whitebark pine. *Oecologia*, *55*(2), 192−201.
Kelly, M., & Meentemeyer, M. K. (2002). Landscape dynamics of the spread of Sudden Oak Death. *Photogrammetric Engineering and Remote Sensing*, *68*, 1001−1009.
Lewis, S. A., Robichaud, P. R., Frazier, B. E., Wu, J. Q., & Laes, D. Y. M. (2008). Using hyperspectral imagery to predict post-wildfire soil water repellency. *Geomorphology*, *95*, 192−205.
Logan, J. A., & Powell, J. A. (2001). Ghost forests, global warming, and the mountain pine beetle. *American Entomologist*, *47*, 160−172.
Logan, J. A., Regniere, J., & Powell, J. A. (2003). Assessing the impacts of global warming on forest pest dynamics. *Frontiers in Ecology and the Environment*, *1*(3), 130−137.
Logan, J. A., White, P., Bentz, B. J., & Powell, J. A. (1998). Model analysis of spatial patterns in mountain pine beetle outbreaks. *Theoretical Population Biology*, *53*(3), 236−255.
Lynch, H. J., Renkin, R. A., Crabtree, R. L., & Moorcroft, P. M. (2006). The influence of previous mountain pine beetle (*Dendroctonus ponderosae*) acitivity on the 1988 Yellowstone fires. *Ecosystems*, *9*, 1318−1327.
Maloy, O. C. (1997). White pine blister rust control in North America: A case history. *Annual Review of Phytopathology*, *35*, 87−109.
Mattson, D. J., Blanchard, B. M., & Knight, R. R. (1991). Food habits of Yellowstone grizzly bears, 1977–1987. *Canadian Journal of Zoology*, *69*(6), 1619−1629.
Mattson, D. J., Blanchard, B. M., & Knight, R. R. (1992). Yellowstone grizzly bear mortality, human habituation, and whitebark pine seed crops. *Journal of Animal Management*, *56*(3), 432−442.
Mielke, J. L. (1943). White pine blister rust in western North America. *Yale University School of Forestry Bulletin*, *vol. 52*. 155 pp.
Miller, J. M., & Keen, F. P. (1960). Biology and control of the western pine beetle. *USDA Miscellaneous Publication No. 800*.
Moeur, M. (1997). Spatial models of competition and dynamics in old-growth Tsuga heterophylla/Thuja plicata forests. *Forest Ecology and Management*, *94*, 175−186.
Moorcroft, P. R., Hurtt, G. C., & Pacala, S. W. (2001). A method for scaling vegetation dynamics: the ecosystem demography model (ED). *Ecological Monographs*, *71*, 557−586.
Mundt, J. T., Glenn, N. F., Weber, K. T., Prather, T. S., Lass, L. W., & Pettingill, J. (2005). Driscrimination of hoary cress and determination of its detection limits via hyperspectral image processing and accuracy assessment techniques. *Remote Sensing of Environment*, *96*, 509−517.
Noujdina, N. V., & Ustin, S. L. (2008). Mapping downy brome (Bromus tectorum) using multidate AVIRIS data. *Weed Science*, *56*, 173−179.
Peterson, C. J., & Squiers, E. R. (1995). An unexpected change in spatial pattern across 10 years in an aspen-white pine forest. *Journal of Ecology*, *83*, 847−855.
Ripley, B. D. (1976). The second-order analysis of stationary point processes. *Journal of Applied Probability*, *13*, 255−266.
Ripley, B. D. (1981). *Spatial statistics*. Chichester, United Kingdom: Wiley.
Robichaud, P. R., Lewis, S. A., Laes, D. Y. M., Hudak, A. T., Kokaly, R. F., & Zamudio, J. A. (2007). Postfire soil burn severity mapping with hyperspectral image unmixing. *Remote Sensing of Environment*, *108*, 467−480.
Roughgarden, J., Running, S. W., & Matson, P. A. (1991). What does remote sensing do for ecology? *Ecology*, *72*, 1918−1922.
Schoettle, A. W., & Sniezko, R. A. (2007). Proactive intervention to sustain high-elevation pine ecosystems threatened by white pine blister rust. *Journal of Forest Research*, *12*, 327−336.
Skakun, R. S., Wulder, M. A., & Franklin, S. E. (2003). Sensitivity of the thematic mapper enhanced wetness difference index to detect mountain pine beetle red-attack damage. *Remote Sensing of Environment*, *86*, 433−443.
Suzuki, R. O., Kudoh, H., & Kachi, N. (2003). Spatial and temporal variations in mortality of the biennial plant, Lysimachia rubida: Effects of intraspecific competition and environmental heterogeneity. *Journal of Ecology*, *91*, 114−125.
Szwagrzyk, J., & Czerwczak, M. (1993). Spatial patterns of trees in natural forests of East-Central Europe. *Journal of Vegetation Science*, *4*, 469−476.
Tomback, D. F. (1982). Dispersal of whitebark pine seeds by Clark's nutcracker: A mutualism hypothesis. *Journal of Animal Ecology*, *51*(2), 451−467.
Tomback, D. F., & Resler, L. M. (2007). Invasive pathogens at alpine treeline: Consequences for treeline dynamics. *Physical Geography*, *28*, 397−418.
Tomback, D. F., Arno, S. F., & Keane, R. E. (2001). The compelling case for management intervention. In D. F. Tomback, S. F. Arno, & R. E. Keane (Eds.), *Whitebark pine communities* (pp. 3−28). Washington, DC: Island Press.
U. S. Geological Survey (USGS). 1999. National Elevation Dataset. EROS Data Center, Sioux Falls, SD.
U. S. Geologial Survey (USGS). 2001. Digital Orthophoto Quadrangles. National Seamless Data Server, http://seamless.usgs.gov/index.php
White, J. C., Wulder, M. A., Brooks, D., Reich, R., & Wheate, R. D. (2004). Mapping mountain pine beetle infestation with high spatial resolution satellite imagery. *Forestry Chronicle*, *80*, 743−745.
Wulder, M. A., Dymond, C. C., White, J. C., Leckie, D. G., & Carroll, A. L. (2006). Surveying mountain pine beetle damage of forests: a review of remote sensing opportunities. *Forest Ecology and Management*, *221*, 27−41.

Please cite this article as: Hatala, J.A., et al., Landscape-scale patterns of forest pest and pathogen damage in the Greater Yellowstone Ecosystem, *Remote Sensing of Environment* (2009), doi:10.1016/j.rse.2009.09.008